SPITZER OBSERVATIONS OF GAMMA-RAY BURST HOST GALAXIES: A UNIQUE WINDOW INTO HIGH-REDSHIFT CHEMICAL EVOLUTION AND STAR FORMATION

R. CHARY,[1] E. BERGER,[2,3,4] AND L. COWIE[5]

ABSTRACT

We present deep 3.6 μm observations of three $z \sim 5$ GRB host galaxies with the *Spitzer Space Telescope*. The host of GRB 060510B, at $z = 4.942$, is detected with a flux density of 0.23 ± 0.04 μJy, corresponding to a rest-frame V-band luminosity of $1.3 \times 10^{10} L_\odot$, or $\approx 0.15 L_{*,V,z=3}$. We do not detect the hosts of GRBs 060223A and 060522 and constrain their rest-frame V-band luminosity to $< 0.1 L_{*,V,z=3}$. Our observations reveal that $z \sim 5$ GRB host galaxies are a factor of ~ 3 less luminous than the median luminosity of spectroscopically confirmed $z \sim 5$ galaxies in the Great Observatories Origins Deep Survey and the Hubble Ultra Deep Field. The strong connection between GRBs and massive star formation implies that not all star-forming galaxies at these redshifts are currently being accounted for in deep surveys and GRBs provide a unique way to measure the contribution to the star formation rate density from galaxies at the faint end of the galaxy luminosity function. By correlating the comoving star formation rate density with comoving GRB rates at lower redshifts, we estimate a lower limit to the star formation rate density of 0.12 ± 0.09 and 0.09 ± 0.05 $M_\odot$ yr^{-1} Mpc^{-3} at $z \sim 4.5$ and $z \sim 6$, respectively. This is in excellent agreement with extinction-corrected estimates from Lyman break galaxy samples. Finally, our observations provide initial evidence that the metallicity of star-forming galaxies evolves more slowly than the stellar mass density between $z \sim 5$ and $z \sim 0$, probably indicative of the loss of a significant fraction of metals to the intergalactic medium, especially in low-mass galaxies.

Subject headings: cosmology: observations — galaxies: abundances — galaxies: high-redshift —
galaxies: starburst — gamma rays: bursts

Online material: color figure

1. INTRODUCTION

Our ability to measure the star formation rate density (SFRD) at $z > 4$ relies almost entirely on either narrowband surveys which detect strong Lyα emitting galaxies (Hu et al. 2004; Nagao et al. 2007) or deep imaging surveys of UV-bright Lyman break galaxies (LBGs; Giavalisco et al. 2004; Bouwens et al. 2006; Hu & Cowie 2006). These surveys, by virtue of being flux limited, trace the bright end of the galaxy luminosity function down to $\sim 0.04 L_{*,UV,z=3}$. The various observations have revealed a decline in the SFRD by about a factor of 3 between $z \sim 3$ and $z \sim 6$ (Bouwens et al. 2006; Bunker et al. 2004), with much of this decline being due to the evolution of the bright end of the galaxy luminosity function.

More than 90% of the estimated SFRD at these redshifts takes place in sub-$L_{*,UV,z=3}$ galaxies. In addition, spectroscopic confirmation of high-redshift galaxies relies on Lyα emission, which is easily obscured by dust. There is now increasing evidence for rapid dust production within ~ 1 Gyr of the big bang (Chary et al. 2007, 2005; Maiolino et al. 2004). As a result, quantifying possible dust extinction corrections and measuring the faint-end slope of the galaxy luminosity function is essential for minimizing uncertainties in the high-redshift SFRD.

Measurements of the metallicity in typical star-forming galaxies at $z > 4$ is beyond the technological capability of the current generation of instrumentation. The relevant rest-frame optical emission lines are very weak and are redshifted to the mid-IR. The alternative approach of studying chemical enrichment through damped Lyα absorbers (DLAs) detected against background quasars appears to be limited to $z \lesssim 5$ (Prochaska et al. 2003; Songaila & Cowie 2002), and is biased toward tracing the properties of extended halo gas, which at lower redshift significantly underestimates the disk metallicity. As a result, the apparent evolution in the mass-metallicity and luminosity-metallicity relations (*M-Z* and *L-Z*) from $z = 0$ to $z \sim 2$ (e.g., Tremonti et al. 2004; Kobulnicky & Kewley 2004; Savaglio et al. 2005) cannot be traced to $z > 5$, where such information should shed light on the initial stages of mass buildup and metal enrichment in galaxies.

Long-duration GRBs, by virtue of being associated with the deaths of massive stars, provide a complementary technique for measuring the SFRD and the chemical enrichment history. *Swift* has revolutionized this study by detecting GRBs out to $z \sim 6$ (Gehrels et al. 2004; Kawai et al. 2006). Prompt spectroscopy of the bright afterglows has now provided a sample of ~ 20 GRBs over a wide range of redshifts with a wealth of metal absorption features arising in the host galaxy (e.g., Jensen et al. 2001; Castro et al. 2003; Hjorth et al. 2003; Vreeswijk et al. 2004; Fynbo et al. 2006). These observations provide a unique window into the metallicity and gas column density in star-forming environments at high redshifts (Chen et al. 2005; Berger et al. 2006; Prochaska et al. 2006, 2007b; Price et al. 2007). Once the afterglows fade away, deep observations of the field can also reveal the stellar mass and SFR of the host galaxies, which can then be correlated with the inferred metallicities.

In order to study the host galaxies of high-redshift GRBs and take advantage of the diagnostics afforded by GRBs, we present *Spitzer Space Telescope* 3.6 μm observations of the hosts of three GRBs at $4 \lesssim z \lesssim 5$. Building on the constraints provided by Berger et al. (2007b) on the host galaxy of GRB 050904 at $z = 6.295$,

[1] *Spitzer* Science Center, California Institute of Technology, Mail Stop 220-6, Pasadena, CA 91125.

[2] Observatories of the Carnegie Institution of Washington, 813 Santa Barbara Street, Pasadena, CA 91101.

[3] Princeton University Observatory, Peyton Hall, Ivy Lane, Princeton, NJ 08544.

[4] Hubble Fellow.

[5] Institute for Astronomy, University of Hawaii, Honolulu, HI 96822.

TABLE 1
Spitzer Observations of $z \sim 5$ GRB Host Galaxies

GRB	R.A. (J2000.0)	Decl. (J2000.0)	Redshift	Date of Observation	Sky Background[a] (MJy sr^{-1})	Exposure Time (s)	Flux Density in μJy 3.6 μm	5.8 μm
GRB 060223A	03 40 49.561	−17 07 48.36	4.406	2006 Sep 23	24.8	130 × 100	<0.3	<2.4
GRB 060510B	15 56 29.607	+78 34 12.42	4.942	2006 Oct 26	13.4	130 × 100	0.23 ± 0.04	<2.1
GRB 060522............	21 31 44.800	+02 53 10.35	5.110	2006 Nov 23	28.4	138 × 100	<0.2	<2.4

Note.—Units of right ascension are hours, minutes, and seconds, and units of declination are degrees, arcminutes, and arcseconds.
[a] Background at 24 μm, dominated by the zodiacal light.

we discuss the nature of the host galaxies and the redshift evolution of the luminosity-metallicity relation and provide an independent measure of the high-redshift SFRD for comparison with estimates from LBG samples. Throughout this paper, we adopt a $\Omega_M = 0.27$, $\Omega_\Lambda = 0.73$, and $H_0 = 71$ km s^{-1} Mpc^{-1} cosmology.

2. OBSERVATIONS

As part of *Spitzer* program GO 20000 (PI: E. Berger) we observed the fields of GRBs 060223A ($z = 4.406$; E. Berger et al. 2008, in preparation), 060510B ($z = 4.942$; Price et al. 2007), and 060522 ($z = 5.110$; E. Berger et al. 2008, in preparation) with the Infrared Array Camera (IRAC; Fazio et al. 2004) in the bandpasses centered at 3.6 and 5.8 μm (Table 1). The observations were undertaken between 2006 September and November, after the afterglows associated with the GRBs had faded below the detectability threshold. As shown in Table 1, the GRB fields lie in regions with "low" to "medium" level zodiacal background and cirrus of 13–28 MJy sr^{-1} at 24 μm on the date of the observations. We used 100 s integrations with about 130 medium scale dithers from the random cycling pattern for total on-source integration times of $\sim$13,000 s at each passband. The nominal 3 σ point source sensitivity limits at 3.6 and 5.8 μm are 0.26 and 2.4 μJy, respectively.

Starting with the S14.4.0 pipeline-processed basic calibrated data (BCD) sets we corrected the individual frames for muxbleed and column pull down using software developed for the Great Observatories Origins Deep Survey (GOODS). Due to the presence of bright stars in the field, many of the frames at 3.6 μm also showed evidence for "muxstriping." This was removed using an additive correction on a column by column basis. The processed BCD frames were then mosaicked together using the MOPEX routine (Makovoz & Khan 2005) and drizzled onto a 0.6$''$ grid. Astrometry was performed with respect to the brightest 2MASS stars in the field which showed a peak-to-peak astrometric uncertainty of 0.2$''$ at 3.6 μm.

The location of the GRB hosts was determined by aligning the *Spitzer* images against images of the afterglow from the *Swift* UV/optical telescope (GRBs 060223A and 060522) and the Gemini Multi-Object Spectrograph on the Gemini-North 8 m telescope (060510B). For the latter, the astrometric uncertainty is 0.09$''$ in each coordinate, while using the UVOT images we obtain an astrometric uncertainty of about 0.6$''$.

All three GRB locations show the presence of nearby (3$''$) brighter galaxies: GRB 060223A has two sources with flux densities of 7.2 and 9.1 μJy at distances of 1.9$''$ and 2.3$''$ from the GRB position; GRB 060510B has a source with a flux of 6.1 μJy about 3.1$''$ from the GRB position; and GRB 060522 has a source with 0.72 μJy located 1.6$''$ away from the burst position. This is not unexpected given the high source density in deep IRAC images. We subtracted the contribution of these sources, in order to obtain the strongest possible constraints on the flux from the GRB host galaxies.

Photometry at the position of the host galaxies was performed in fixed circular apertures of 1.2$''$ radius with appropriate beam-size corrections applied as stated in the *Spitzer* Observer's Manual. We clearly detect a galaxy coincident with the position of GRB 060510B with a flux density of 0.23 ± 0.04 μJy at 3.6 μm, and a 3 σ upper limit of 2.1 μJy at 5.8 μm (Fig. 1). For GRBs 060223A and 060522, due to blending from nearby brighter sources and the residual effects from muxbleed, we are only able to provide 3 σ upper limits to the flux of the host galaxy (Table 1).

3. LUMINOSITY AND METALLICITY OF GRB HOSTS

Of the four GRB host galaxies at $z \sim 5$ observed in this program at 3.6 and 5.8 μm (including GRB 050904), only GRB 060510B is clearly detected. The observed 3.6 μm flux densities/limits for these galaxies correspond to rest-frame V-band luminosities of $\sim$0.15 $L_{*,V,z=3}$, where $L_{*,V,z=3}$ is about $8 \times 10^{10} L_\odot$ (Marchesini et al. 2007; Shapley et al. 2001). It is illustrative to compare the properties of GRB hosts with the field galaxy population at similar redshifts.

The GOODS fields have extensive spectroscopy of galaxies at high redshift (Vanzella et al. 2005, 2006; E. Vanzella et al. 2008, in preparation). There are 275 LBGs in both the GOODS fields, which are classified as V-band "dropouts," i.e., $z \sim 5$. The magnitude limit of the GOODS optical observations imply that they are brighter than $\sim$0.2 $L_{*,\mathrm{UV},z=3}$ (Giavalisco et al. 2004). Of these, $\sim$20% have spectroscopic redshifts, while $\sim$30% are individually detected with IRAC. At higher redshifts, $z \sim 6$, it has been shown that galaxies which are individually undetected with IRAC appear to harbor a younger stellar population and have a factor of 10 lower stellar mass than IRAC-detected galaxies (Yan et al. 2006).

As shown in Figure 2, GRB host galaxies are factors of 2–3 times fainter than the median V-band luminosity of galaxies which have spectroscopic redshifts of $4.5 < z < 5.5$ in the GOODS field. Furthermore, the luminosities are comparable to the rest-frame V-band luminosity of GRB hosts studied at lower redshifts (e.g., Chary et al. 2002; Le Floc'h et al. 2003). This suggests that GRB host galaxies are unlike the luminous end of the star-forming, LBG population which have had more than a factor of 10 increase in their stellar mass between $z \sim 5$ and $z \sim 1$. They are more typical of the blue, faint end of the galaxy V-band luminosity function, a population for which it is difficult to measure redshifts or metallicities, in the absence of GRBs, due to their inherent faintness.

GRB host galaxies at $z \sim 0.5$–3, which have extensive multi-wavelength data, show clear evidence for very high specific SFRs indicating an on-going starburst (Chary et al. 2002; Christensen et al. 2004; Castro Cerón et al. 2006). We do not yet have constraints on the SFRs in the $z \sim 5$ host galaxies presented here, due to their intrinsic faintness in the rest-frame UV (see, e.g., Fruchter et al. 2006; Jakobsson et al. 2005). However, spectroscopy of the afterglows by Price et al. (2007) and E. Berger et al. (2008, in
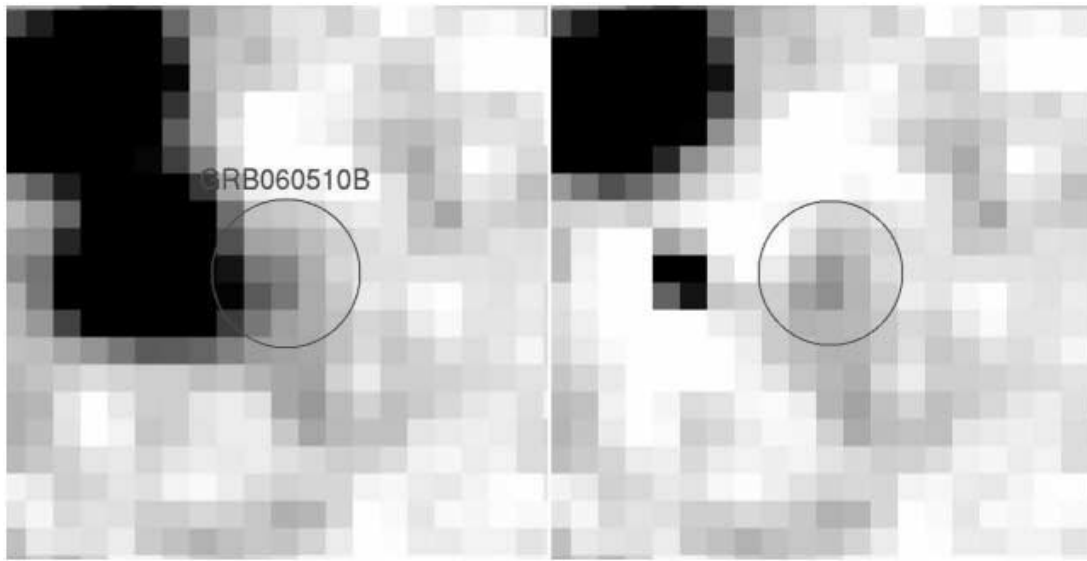
Fig. 1.—*Spitzer* image of the host galaxy of GRB 060510B at $15^h56^m29.607^s$, $+78°34'12.42''$ (J2000.0). Image is $12''$ on a side; north is up, and east is to the left. The left panel shows the processed mosaic, while the right panel shows the image with the foreground galaxy $3.1''$ to the east subtracted. [*See the electronic edition of the Journal for a color version of this figure.*]

preparation) has revealed a wealth of absorption lines which have been used to derive the metallicity and gas column density in the vicinity of the burst.

Absorption spectroscopy of the three bursts presented here has yielded neutral hydrogen gas densities in their host galaxies of $\log [N(\text{H I})] = 21.6 \pm 0.1$ (GRB 060223A), $\log [N(\text{H I})] = 21.3 \pm 0.1$ (GRB 060510B), and $\log [N(\text{H I})] = 21.0 \pm 0.3$ (GRB 060522). Thus, all three systems are clearly DLAs, with column densities near the median of the distribution for GRB-DLAs (Berger et al. 2006; Jakobsson et al. 2006). In addition, the metallicities of the GRBs 060223A and 060510B systems have been determined from the detection of weak metal lines. For GRB 060522 the signal-to-noise ratio of the spectrum is too low to clearly identify any metal lines and an estimate of the metallicity is thus not possible. In the case of GRB 060223A, we find an upper limit on the column density of S II of $\log [N(\text{S II})] < 15.3$, leading to a metallicity of $[\text{S/H}] < -1.45$. The nondetection of Fe II $\lambda1608$

leads to a limit of $[\text{Fe/H}] < -2.65$, but we stress that iron can be heavily depleted onto dust grains. From the detection of the Si II $\lambda1304$ line we find $\log [N(\text{Si II})] \approx 15.3$, and hence $[\text{Si/H}] \approx -1.8$. As in the case of iron, silicon is also strongly depleted, so we conclude that the metallicity of the GRB 060223A DLA is in the range -1.8 to -1.4. For GRB 060510B, we use the S II $\lambda\lambda1250, 1253$ lines to measure $\log [N(\text{S II})] = 15.6 \pm 0.1$, and hence a metallicity $[\text{S/H}] = -0.85 \pm 0.15$ (see also Price et al. 2007).

The metallicity estimates of the GRB hosts along with their rest-frame *B*-band luminosities (assuming a $B - V$ color of 0, typical of star-forming galaxies) are shown in Figure 3. Also shown for comparison are the metallicity-luminosity relationships for different samples of field galaxies. Despite the one detection and two limits for the luminosity of the host galaxies, the figure shows that the redshift evolution of metallicity at a fixed *B*-band luminosity that is seen in the range $0 < z < 2$ clearly extends out to $z \sim 5$.
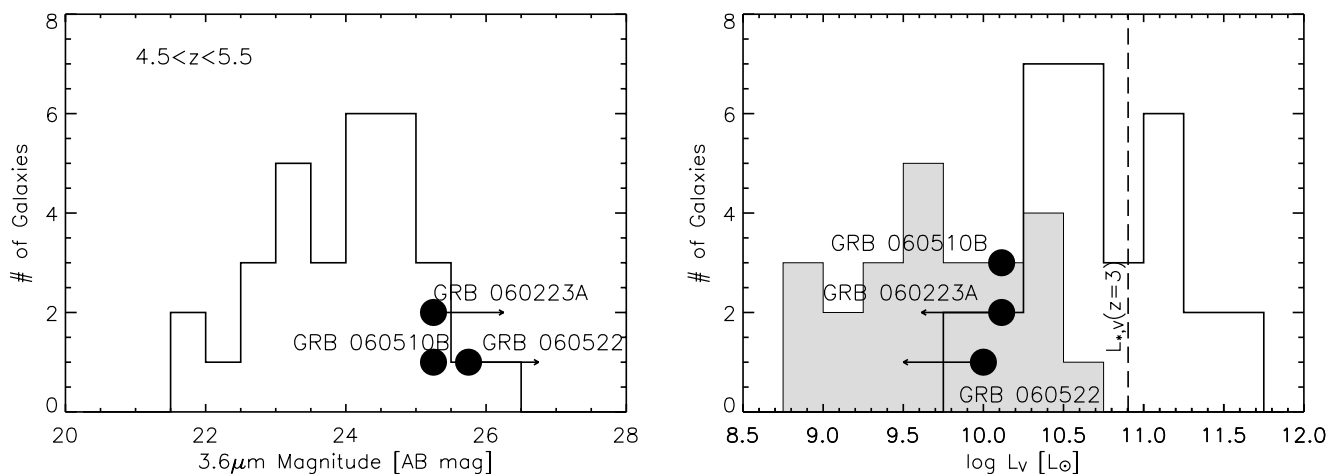

Fig. 2.—*Left*: Histogram showing the distribution of observed 3.6 μm magnitudes for galaxies in the GOODS fields with spectroscopic redshifts $4.5 < z < 5.5$. The solid symbols show the brightness of the GRB host galaxies observed in this paper relative to the field galaxies. *Right*: GRB hosts have rest-frame *V*-band luminosities which are a factor of ~2–3 fainter than field galaxies at similar redshifts and provide a complementary way to study the faint-end luminosity function of star-forming galaxies. Also shown as the shaded histogram are the *V*-band luminosities of GRB hosts at a median redshift of ~1 (Chary et al. 2002; Le Floc'h et al. 2003), which indicate that GRB hosts span similar *V*-band luminosities, regardless of redshift.
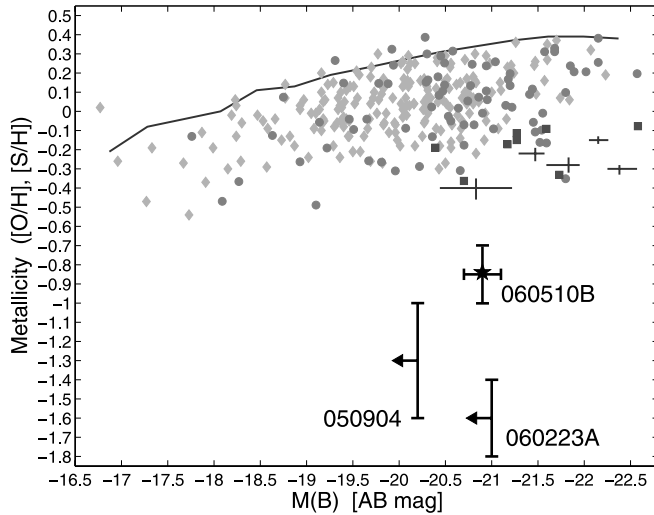
FIG. 3.—Luminosity-metallicity relationship for star-forming galaxies at $z < 2$ compared with the host galaxies of $z > 4$ gamma-ray bursts. The galaxy data are from the Gemini Deep Deep Survey and the Canada-France Redshift Survey at $z \sim 0.4–1$ (*circles*; Savaglio et al. 2005), the Team Keck Redshift Survey at $z \sim 0.3–1$ (*diamonds*; Kobulnicky & Kewley 2004), DEEP2 at $z \sim 1–1.5$ (*squares*; Shapley et al. 2005), and LBGs at $z \sim 2.3$ (*error bars*; Erb et al. 2006). The gray lines represent the relation derived for $z \sim 0.1$ galaxies from the Sloan Digital Sky Survey (Tremonti et al. 2004). GRBs provide a unique window into the evolution of the mass-metallicity relation at high redshift and indicate that the chemical enrichment of galaxies with redshift occurs at a lower rate than the buildup of stellar mass, presumably due to the expulsion of metals in low-mass galaxies by outflows.

The chemical enrichment of galaxies is directly related to their past history of star formation, since supernovae and stellar winds are responsible for recycling the products of nucleosynthesis back into the interstellar medium. The stellar mass density is the time integral of the star formation history. By comparing the redshift evolution of the stellar mass density (ρ_*) (e.g., Dickinson et al. 2003; Yan et al. 2006; Stark et al. 2007; Chary et al. 2007) with the redshift evolution of the metallicity (Z), we can search for evolution of the stellar initial mass function and assess the role of feedback in the buildup of galaxies. The *Spitzer* observations of the hosts are crucial, since they enable metallicity comparisons to be made at a fixed rest-frame V-band luminosity, over a wide range of redshifts.

Due to the fact that we have constraints on the V-band luminosity and metallicity of only one $z \sim 5$ GRB host, we make the assumption that the median metallicity at each redshift is that of a galaxy which has a luminosity similar to that of the GRB host. This is not an unreasonable assumption. Within the observational uncertainties, the slope of the mass-metallicity relation appears to be invariant between $z \sim 0$ and $z \sim 2$ (Erb et al. 2006). The metallicity values are obtained by effectively making a vertical cut at -20.8 mag in Figure 3 and are determined to be -0.85 ± 0.15, -0.35 ± 0.1, and 0.33 ± 0.1 dex at redshifts of 5, 2.3, and 0, respectively. The average estimated ρ_* at these redshifts are 1.4, 6, and 56 in units of $10^7 M_\odot$ Mpc^{-3} (see references above). We performed a Monte Carlo analysis to obtain the best fit between $Z(z)$ and $\rho_*(z)$.

Star-forming galaxies which fall on the local mass-metallicity relationship show a scatter of ~ 0.1 dex at bright luminosities and ~ 0.2 dex at faint luminosities (Tremonti et al. 2004). We use a random number generator to offset the stellar mass density and metallicity by the observed scatter from the mean values quoted above (see Table 3 of Dickinson et al. [2003] for the range in stellar mass density). We fit for the relation between $Z(z)$ and $\rho_*(z)$ and

repeat the process 10,000 times. We find that $dZ/d\rho_*$ appears to be invariant in the range $0 < z < 5$ and that $Z(z) \propto \rho_*(z)^{0.69 \pm 0.17}$. This suggests that the chemical enrichment of star-forming galaxies takes place at a slower rate than the buildup of stellar mass. This is presumably due to the loss of metals from low-mass galaxies by outflows and stellar winds, an effect which is primarily responsible for the mass-metallicity relation seen in the local universe (Tremonti et al. 2004) and $z \sim 2$ LBGs (Erb et al. 2006). However, alternate mechanisms such as depletion of metals onto dust grains cannot be ruled out at this time.

There is the possibility of a selection effect in this analysis. If long-duration GRBs arise in collapsars, they might preferentially be in low-metallicity galaxies. As a result, it is possible that GRB hosts have a lower metallicity than the average field galaxy of the same rest-frame optical luminosity. Although GRB hosts appear to be have low luminosities in the rest-frame UV and V-band, the observational evidence does not indicate that the hosts have an unusually low metallicity for their luminosity. The metallicity of GRB host galaxies appear to span the range 0.1–1 $Z_{\rm solar}$ (e.g., Berger et al. 2007a, 2006; Prochaska et al. 2007a), and some of the hosts have even been found to be associated with dusty, IR-luminous galaxies (e.g., Le Floc'h et al. 2006).

Nevertheless, we assess the reliability of our derived $Z(z)$-$\rho_*(z)$ relation by considering a bias in the metallicity of GRB environments. If we assume that the metallicity of the GRB environment is higher by >0.3 dex compared to the mean metallicity of a galaxy at its luminosity, it implies that the mean metallicity at $z \sim 5$ for a field galaxy at the luminosity of the GRB host is -1.15 ± 0.15. The best-fit relation to the three points is then consistent with an exponent of unity, i.e., $Z(z) \propto \rho_*(z)^{0.85 \pm 0.19}$ but has a worse χ^2. The corollary is that if GRB hosts were biased by 0.3 dex toward lower metallicities, compared to the mean metallicity of a galaxy at its luminosity, the best-fit relation is $Z(z) \propto \rho_*(z)^{0.52 \pm 0.16}$, which is a larger deviation from unity. Furthermore, if there were a bias in GRB host metallicities, the slope of the $Z(z)$-$\rho_*(z)$ relation derived above at a fixed B-band luminosity would have a different value between $2 < z < 5$ and $0 < z < 2$ due to the fact that the $0 < z < 2$ relation is determined from star-forming galaxies, while the $2 < z < 5$ relation is derived from GRB hosts and LBGs. This is inconsistent with our fits, although larger samples of GRB hosts are needed to eliminate suggestions of bias.

Detection of individual GRB hosts at high redshifts is likely to remain difficult, due to their intrinsic faintness. There is a clear need for homogeneous IR surveys of GRB host galaxies which will enable stacking to be performed as a function of metallicity, gas density, and rest-frame UV properties. Within our sample, GRB 050904 is a marginal IRAC detection (Berger et al. 2007b), while GRB 060223A is dominated by detector systematics. As a result, we are unable to provide additional constraints using stacking. Observations of a larger sample of GRB hosts, such as those currently being targeted in *Spitzer* program GO4-40599 (PI: R. Chary), will allow the luminosity-metallicity relation to be measured at high redshift and lead to a better understanding of the faint end of the galaxy luminosity function, a regime which is currently inaccessible even through ultradeep surveys like GOODS and the UDF.

4. EVOLUTION OF THE STAR FORMATION RATE DENSITY

It is now well known from various mid-IR, far-IR, and submillimeter surveys that the SFRD at $z \sim 0.5–2.5$ is dominated by IR-luminous galaxies with $L_{\rm IR} = L(8–1000 \ \mu{\rm m}) > 10^{11} \ L_\odot$ and $L_{\rm IR}/L_{\rm UV} \sim 10–100$ (e.g., Takeuchi et al. 2005; Burgarella et al. 2006; Chary & Elbaz 2001). At $z \gtrsim 3$, current long-wavelength

surveys, due to their limited sensitivity, are unable to detect galaxies which harbor the bulk of the star formation. Thus, rest-frame UV observations of galaxies are the only avenue for probing star formation at high redshifts.

The primary uncertainties associated with quantifying the SFRD at $z > 3$ are the contribution from galaxies at the faint end of the UV-luminosity function and dust corrections. Since sub-$L_{*,\mathrm{UV},z=3}$ galaxies contribute $\sim$90% of the SFRD, measurement of the faint-end slope of the UV luminosity function, where completeness corrections and surface brightness dimming issues are significant, needs to be undertaken carefully (Steidel et al. 1999; Bouwens et al. 2006). Similarly, if extinction were a significant issue, the galaxies that dominate the SFRD would be UV-faint or undetected in magnitude-limited rest-frame UV surveys. GRBs are relatively insensitive to these limitations. If the GRB rate density were correlated with the comoving SFRD at lower redshifts, where cross-calibration between the UV and IR are in broad agreement, measurement of the GRB rate density at $z > 3$ could provide an independent pathway to quantifying the SFRD (see also, e.g., Price et al. 2006).

The three parameters which are most likely to dominate the calibration between GRBs and the SFRD are the evolution of metallicity with redshift, the evolution of the initial mass function of stars, and the identification and spectroscopic follow-up of the GRB afterglow. If long-duration GRBs were to preferentially occur in low-metallicity environments, the increase in the average metallicity of the universe with decreasing redshift would result in a higher SFR/GRB-rate ratio at low redshift. Similarly, evolution of the stellar initial mass function from a "top-heavy" to a Salpeter mass function with decreasing redshift would increase the SFR/GRB-rate ratio at low redshift. On the other hand, the detection efficiency and spectroscopic completeness of GRBs should be increasing with decreasing redshift, implying a lower SFR/GRB-rate ratio at low redshift.

Calibrating each of these parameters individually is challenging at the present time, partly because the relationship between GRB rate and environment is not well known and partly due to the fact that observational selection effects cannot be quantified. Therefore, we need to rely on empirical comparisons between known SFR estimates and GRB rate densities to assess GRBs as a SFR indicator. This empirical comparison can be optimally done at $z < 3$, since in this redshift range the SFR, including the dust obscured component, has been accurately determined from deep mid-IR and submillimeter surveys.

We use the SFRD at $z < 3$ from Chary & Elbaz (2001). We distribute the 52 *Swift* GRBs with spectroscopic redshifts into redshift bins and divide by the comoving volume in each redshift bin. We also correct for the time dilation to estimate the comoving GRB rate density over the $\sim$2 yr *Swift* lifetime. The redshift bin at $z < 0.5$ is omitted, since the GRB rate density appears to be anomalously high compared to the rapidly evolving SFRD. We find that within the uncertainties, the rate density of GRBs with spectroscopic redshifts in the range $0.5 < z < 3$ is constant at a value of $(3.7 \pm 1.1) \times 10^{-11}$ Mpc^{-3} yr^{-1}. This can be compared with the extinction-corrected comoving SFRD in the same redshift range, which is in the range 0.12–0.25 $M_\odot$ yr^{-1} Mpc^{-3} and has an average value of $\sim$0.2 $M_\odot$ yr^{-1} Mpc^{-3} (Chary & Elbaz 2001).

Since these two independent rate densities are relatively constant in the $0.5 < z < 3$ range, we can tentatively make the assumption that the SFR/GRB-rate is constant (Fig. 4). The ratio of these two rates implies

$$\mathrm{SFRD} = \mathrm{GRB\ rate} \times (5.2 \pm 2.3) \times 10^9, \qquad (1)$$
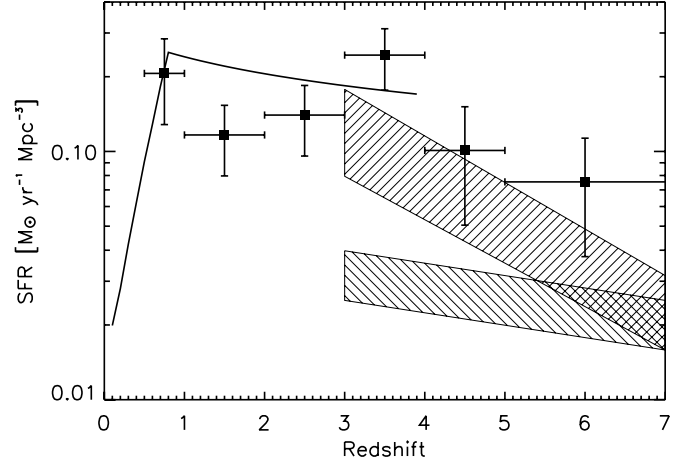

Fig. 4.—SFRD inferred from spectroscopically confirmed long-duration *Swift* GRBs (*squares*). The solid black line is the extinction-corrected SFRD inferred at $z < 4$ from a variety of multiwavelength surveys in the mid-IR and submillimeter, which are used to calibrate the GRBs (Chary & Elbaz 2001). The lower hatched region is the extinction-uncorrected SFRD from rest-frame UV surveys ($>0.04\,L_{*,\mathrm{UV},z=3}$), including estimates by Steidel et al. (1999), Yoshida et al. (2006), and Bouwens et al. (2006). The upper hatched shape contains these values corrected upward for reddening using the UV-slope technique by Bouwens et al. (2006). The SFRD inferred from GRBs at $z > 4$ is consistent, within the significant errors, to the extinction-corrected SFRD. Follow-up of a larger number of high-redshift GRBs is required to confirm if the higher rate density derived from the GRBs is statistically significant.

where SFRD is the extinction-corrected SFRD in $M_\odot$ yr^{-1} Mpc^{-3} and GRB rate is in units of Mpc^{-3} yr^{-1}.

Using our derived calibration, and the measured GRB rate densities at $4 < z < 5$ and $5 < z < 7$ of $(2.4 \pm 1.2) \times 10^{-11}$ and $(1.8 \pm 0.9) \times 10^{-11}$ Mpc^{-3} yr^{-1}, respectively, we infer a net SFR, corrected for extinction, of 0.12 ± 0.06 and 0.09 ± 0.05 $M_\odot$ yr^{-1} Mpc^{-3} at $z \sim 4.5$ and $z \sim 6$, respectively. These estimates are systematically higher than those derived by Price et al. (2006) by factors of 3–5. The Price et al. (2006) estimates were calibrated at $z \sim 3$, where neither the completeness correction factor for the faint end of the UV luminosity function nor the dust extinction correction are reliably known, while deep *Spitzer* mid-IR surveys have confirmed the dominant contribution of IR luminous galaxies to the SFRD at $0.5 < z < 3$ (Takeuchi et al. 2005; Daddi et al. 2007). The fact that the GRB rate density is almost flat in the range $0.5 < z < 6$, while parameters such as the detection efficiency and spectroscopic completeness should be decreasing with increasing redshift, implies that the measured GRB rate density provides at least a lower limit to the SFRD.

It is illustrative to compare this SFR estimate with those from deep rest-frame UV surveys at $z > 4$. Giavalisco et al. (2004) derive a SFRD at $z \sim 4$ of 0.02 $M_\odot$ yr^{-1} Mpc^{-3} when integrating to $0.2\,L_{*,\mathrm{UV},z=3}$. After application of an extinction correction of $A_V = 0.45$ mag, based on the extinction properties in local starburst galaxies, they estimate the total SFRD at $z \sim 4$ to be 0.15 $M_\odot$ yr^{-1} Mpc^{-3}. Similarly, Bouwens et al. (2006) derive a SFRD at $z \sim 6$ by integrating the luminosity function of LBGs in the UDF and other deep fields. Integrating the UV luminosity function down to $0.2\,L_{*,\mathrm{UV},z=3}$ results in a value of 1.3×10^{-2} $M_\odot$ yr^{-1} Mpc^{-3}, while the integral to $10^7\,L_\odot$ yields a SFRD of 0.04 $M_\odot$ yr^{-1} Mpc^{-3}. Application of an extinction correction, inferred to be about $A_{\mathrm{UV}} = 0.45$ mag at $z \sim 6$, to this latter number implies a SFRD of 0.06 $M_\odot$ yr^{-1} Mpc^{-3}.

The agreement between the SFRD values estimated from UV surveys and the GRB rate density is reassuring, considering that there have been only eight GRBs that have been spectroscopically

confirmed to be at $z > 4$ (Fig. 4). However, the SFRD from GRBs primarily traces the faint end of the galaxy luminosity function while the surveys are measuring the contribution from the bright end. As a result, a more reasonable SFRD estimate requires adding the SFRD contribution estimated from the faint end of the galaxy luminosity function, from GRBs, to that from bright LBGs.

GRB hosts are fainter than $0.2 L_{*,V,z=3}$. Based on the UV to V-band flux ratios of star-forming galaxies at $z \sim 3$, it implies that GRB hosts must be fainter than $0.2 L_{*,UV,z=3}$. Adding the SFRD from $L > 0.2 L_{*,UV,z=3}$ galaxies to that inferred from the GRB rate density results in an extinction-corrected SFRD of 0.27 ± 0.13 and $0.11 \pm 0.05 M_\odot$ yr^{-1} Mpc^{-3} at $z \sim 4.5$ and $z \sim 6$, respectively. If confirmed through a larger statistical sample, this is a substantial upward revision suggesting that $L < 0.2 L_{*,UV,z=3}$ galaxies contribute at least 4 times as much to the SFRD at $z \sim 6$ as the bright end ($L > 0.2 L_{*,UV,z=3}$) of the UV luminosity function. Indirectly, this implies that the faint-end slope of the UV luminosity function at $z \sim 6$ must be approximately -1.9, compared to the value of -1.73 that was derived by Bouwens et al. (2006).

GRBs are a powerful tool for measuring the high-redshift SFRD. In particular, deep *Spitzer* observations of GRB hosts can reveal the contribution to the SFRD from the faint end of the galaxy luminosity function, a regime which is inaccessible to deep, rest-frame UV/near-IR surveys. Increasing the sample of high-redshift GRBs will reduce the uncertainties in the SFRD unaffected by extinction, and through stacking analysis on the host galaxies will help estimate the contribution to the stellar mass density from sub-L_* galaxies. Comparison between SFR estimates from GRBs with those from deep UV surveys will provide better constraints on the evolution of dust extinction at high redshift and provide tremendous insights into the chemical enrichment of the early universe.

REFERENCES

Berger, E., Fox, D. B., Kulkarni, S. R., Frail, D. A., & Djorgovski, S. G. 2007a, ApJ, 660, 504
Berger, E., Penprase, B. E., Cenko, S. B., Kulkarni, S. R., Fox, D. B., Steidel, C. C., & Reddy, N. A. 2006, ApJ, 642, 979
Berger, E., et al. 2007b, ApJ, 665, 102
Bouwens, R. J., Illingworth, G. D., Blakeslee, J. P., & Franx, M. 2006, ApJ, 653, 53
Bunker, A. J., Stanway, E. R., Ellis, R. S., & McMahon, R. G. 2004, MNRAS, 355, 374
Burgarella, D., et al. 2006, A&A, 450, 69
Castro, S., Galama, T. J., Harrison, F. A., Holtzman, J. A., Bloom, J. S., Djorgovski, S. G., & Kulkarni, S. R. 2003, ApJ, 586, 128
Castro Cerón, J. M., Michałowski, M. J., Hjorth, J., Watson, D., Fynbo, J. P. U., & Gorosabel, J. 2006, ApJ, 653, L85
Chary, R., Becklin, E. E., & Armus, L. 2002, ApJ, 566, 229
Chary, R., & Elbaz, D. 2001, ApJ, 556, 562
Chary, R.-R., Stern, D., & Eisenhardt, P. 2005, ApJ, 635, L5
Chary, R., et al. 2007, ApJ, submitted
Chen, H.-W., Prochaska, J. X., Bloom, J. S., & Thompson, I. B. 2005, ApJ, 634, L25
Christensen, L., Hjorth, J., & Gorosabel, J. 2004, A&A, 425, 913
Daddi, E., et al. 2007, ApJ, in press
Dickinson, M., Papovich, C., Ferguson, H. C., & Budavári, T. 2003, ApJ, 587, 25
Erb, D. K., Shapley, A. E., Pettini, M., Steidel, C. C., Reddy, N. A., & Adelberger, K. L. 2006, ApJ, 644, 813
Fazio, G. G., et al. 2004, ApJS, 154, 10
Fruchter, A. S., et al. 2006, Nature, 441, 463
Fynbo, J. P. U., et al. 2006, A&A, 451, L47
Gehrels, N., et al. 2004, ApJ, 611, 1005
Giavalisco, M., et al. 2004, ApJ, 600, L103
Hjorth, J., et al. 2003, ApJ, 597, 699
Hu, E. M., & Cowie, L. L. 2006, Nature, 440, 1145
Hu, E. M., Cowie, L. L., Capak, P., McMahon, R. G., Hayashino, T., & Komiyama, Y. 2004, AJ, 127, 563
Jakobsson, P., et al. 2005, MNRAS, 362, 245
———. 2006, A&A, 460, L13
Jensen, B. L., et al. 2001, A&A, 370, 909

Kawai, N., et al. 2006, Nature, 440, 184
Kobulnicky, H. A., & Kewley, L. J. 2004, ApJ, 617, 240
Le Floc'h, E., Charmandaris, V., Forrest, W. J., Mirabel, I. F., Armus, L., & Devost, D. 2006, ApJ, 642, 636
Le Floc'h, E., et al. 2003, A&A, 400, 499
Maiolino, R., Schneider, R., Oliva, E., Bianchi, S., Ferrara, A., Mannucci, F., Pedani, M., & Roca Sogorb, M. 2004, Nature, 431, 533
Makovoz, D., & Khan, I. 2005, in ASP Conf. Ser. 347, Astronomical Data Analysis Software and Systems XIV, ed. P. Shopbell, M. Britton, & R. Ebert (San Francisco: ASP), 81
Marchesini, D., et al. 2007, ApJ, 656, 42
Nagao, T., et al. 2007, A&A, 468, 877
Price, P. A., Cowie, L. L., Minezaki, T., Schmidt, B. P., Songaila, A., & Yoshii, Y. 2006, ApJ, 645, 851
Price, P. A., et al. 2007, ApJ, 663, L57
Prochaska, J. X., Chen, H.-W., & Bloom, J. S. 2006, ApJ, 648, 95
Prochaska, J. X., Chen, H.-W., Dessauges-Zavadsky, M., & Bloom, J. S. 2007a, ApJ, 666, 267
Prochaska, J. X., Gawiser, E., Wolfe, A. M., Castro, S., & Djorgovski, S. G. 2003, ApJ, 595, L9
Prochaska, J. X., et al. 2007b, ApJS, 168, 231
Savaglio, S., et al. 2005, ApJ, 635, 260
Shapley, A. E., Coil, A. L., Ma, C.-P., & Bundy, K. 2005, ApJ, 635, 1006
Shapley, A. E., Steidel, C. C., Adelberger, K. L., Dickinson, M., Giavalisco, M., & Pettini, M. 2001, ApJ, 562, 95
Songaila, A., & Cowie, L. L. 2002, AJ, 123, 2183
Stark, D. P., Bunker, A. J., Ellis, R. S., Eyles, L. P., & Lacy, M. 2007, ApJ, 659, 84
Steidel, C. C., Adelberger, K. L., Giavalisco, M., Dickinson, M., & Pettini, M. 1999, ApJ, 519, 1
Takeuchi, T. T., et al. 2005, A&A, 440, L17
Tremonti, C. A., et al. 2004, ApJ, 613, 898
Vanzella, E., et al. 2005, A&A, 434, 53
———. 2006, A&A, 454, 423
Vreeswijk, P. M., et al. 2004, A&A, 419, 927
Yan, H., Dickinson, M., Giavalisco, M., Stern, D., Eisenhardt, P. R. M., & Ferguson, H. C. 2006, ApJ, 651, 24
Yoshida, M., et al. 2006, ApJ, 653, 988